BOLETIN DE LA SOCIEDAD ESPAÑOLA DE
Cerámica y Vidrio
www.elsevier.es/bsecv

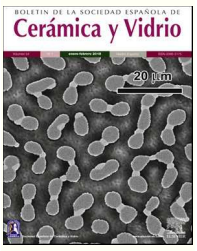

Synthesis and photocatalytic characterisation of mesoporous TiO_2 films doped with Ca, W and N

Yolanda Castro, Noemi Arconada and Alicia Durán*

Instituto de Cerámica y Vidrio (CSIC), Madrid, Spain

ARTICLE INFO

Article history:
Received 12 November 2014
Accepted 23 January 2015

Keywords:
Mesoporous TiO_2 films
Sol-gel coatings
Dopants
Photocatalysis
Degradation of methyl orange

A B S T R A C T

Mesoporous TiO_2 films doped with Ca^{2+}, W^{6+} and nitrogen were obtained by sol-gel method using dip-coating procedure onto glass-slides in order to study the influence of dopants in their textural properties and photocatalytic activity. Titania sols were synthesized with and without dopants using titanium isopropoxide as titanium precursor, two complexing agents, acetic acid and acetyl acetone, and two pore generating agents, Pluronic F-127 (F127) and polyethylene glycol hexadecyl ether (Brij58). Films were characterised by Fourier Transform Infrared Spectroscopy (FTIR), Grazing X-ray diffraction (GXRD) and Transmission Electron Microscopy (TEM). Environmental Ellipsometric Porosimetry (EEP) permitted to obtain the adsorption/desorption isotherms and total pore volume, and to determine the porous size distribution and specific surface area (S_s) of the films. The photocatalytic activity was evaluated through the degradation of methyl orange (MO) in aqueous solution under UV light exposure. The photocatalytic activity depends on the nature of dopants, which affect the TiO_2-anatase crystallite size and the textural properties of the final material. The best results of MO degradation were obtained for the films doped with Ca^{2+}, this being correlated with the pore size and specific surface area of the films besides the dopant-effect on the photocatalytic mechanisms.

Síntesis y caracterización fotocatalítica de recubrimientos mesoporosos de TiO_2 dopados con Ca, W and N

Palabras clave:
Recubrimientos mesoporosos TiO_2
Recubrimientos por sol-gel
Dopantes

R E S U M E N

Se prepararon recubrimientos de TiO_2 mesoporosos dopados con Ca^{2+}, W^{6+} y nitrógeno por el método sol-gel sobre porta objetos de vidrio utilizando la técnica de inmersión, con objeto de estudiar la influencia de los dopantes en las propiedades texturales y fotocatalíticas. Se prepararon soles de titania con y sin dopantes utilizando isopropóxido

* *Corresponding author.*
E-mail address: castro@icv.csic.es (Y. Castro).

http://dx.doi.org/10.1016/j.bsecv.2015.02.003

Fotocatálisis
Degradación de naranja de metilo

de titanio como precursor de titanio, dos agentes complejantes, ácido acético y acetona acetilo, y dos surfactantes, Pluronic F-127 (F127) y éter hexadecil polietilenglicol (Brij58). Los recubrimientos se caracterizan por Espectroscopia Infrarroja de Transformada de Fourier (FTIR), Difracción de Rayos X a bajo ángulo (GXRD) y Microscopía Electrónica de Transmisión (MET). Mediante estudios de Elipsometría Espectral Porosimetrica (EEP) se obtuvieron las isotermas de adsorción/desorción y el volumen total de poro, junto con la distribución del tamaño de poro y la superficie específica (Ss) de los recubrimientos. Los estudios de actividad fotocatalítica se realizaron a través de la descomposición de naranja de metilo bajo irradiación con luz UV/vis. La actividad fotocatalítica depende de la naturaleza del dopante, el cual afecta al tamaño de cristal de TiO_2 anatasa y a las propiedades texturales del material final. Los mejores resultados de la degradación de MO se obtuvieron para los recubrimientos dopadas con Ca^{2+}, que corresponde con un adecuado tamaño de poro y superficie específica, además de las características específicas del dopante.

Introduction

Titanium dioxide in its anatase phase is widely used as a semiconductor photo-catalyst because of its long-term stability, no toxicity and good photocatalytic activity.[1] For an effective photoexcitation of TiO_2 semiconductor it is necessary the illumination with light with energy higher than the titania-anatase band gap ($E_{band\text{-}gap}$), around 3.2 eV; therefore the absorption threshold corresponds to 380 nm. Consequently, only the ultraviolet fraction of the solar irradiation, about 5%, is active in the photoexcitation processes.[2] On the other hand, the recombination of photogenerated electron-hole pairs results in low photoquantum efficiency.[3]

In recent years, the doping of TiO_2 with transition metal ions (Cr, V, Fe, W, etc.)[4] and non-metallic elements (N, F, C, S, B, etc.) has been extensively investigated with the aim of increasing the photocatalytic activity under visible light and full solar light irradiation by introducing additional energy levels in the band gap of TiO_2. Choi et al.[5] carried out a systematic investigation of the photocatalytic efficiency of TiO_2 doped with 21 different metal ions. They report that the efficiency of a dopant depends on different parameters such as the concentration and distribution of the dopant in the matrix of TiO_2, the creation of additional energy levels in the band gap, the electron donor concentration, etc. For example, an excess of dopant concentration could produce a detrimental effect decreasing the photocatalytic activity, because the charge recombination is favoured.[5,6]

The most popular transition metals used as dopants are W, Cr, Fe, Co, Mn and Cu[5] which modify the optical and photo-electrochemical properties of TiO_2, shifting the light absorption of TiO_2 to the visible region and prolonging the lifetime of electron and holes, thus increasing the photocatalytic activity.[7] Particularly, tungsten (W) is found to inhibit the recombination of photoinduced e^-/h^+.[8] Rampaul et al.[9] and Yang et al.[8] evidenced the efficiency of photocatalytic oxidation through W-TiO_2 doped films. The effect of dopant is to create additional intermediate energy levels that modify the electrical and optical properties of the TiO_2 matrix.

On the other hand, the photocatalytic properties of TiO_2 are modified when doped with alkaline and alkaline-earth ions. Al-Salim et al.[10] considered that the photocatalytic activity of TiO_2 films doped with Ca^{2+} increases due to Ca^{2+} ions could be isomorphously substituted or interstitially introduced into the matrix producing oxygen vacant matrix or interstitial Ti^{3+} deforming the TiO_2. The concentration of active sites improves and the recombination of h^+/e^- pairs is avoided. This is the most plausible explanation to the photocatalytic enhance produced by Ca, although we have not found a clear justification in the consulted literature.

Asahi et al.[11] showed that the doping with anionic species (C, N, S, P and F) could replace O in the TiO_2 matrix and thus narrow the band gap. In particular, doping with nitrogen (N-doped) may affect the band-gap structure by mixing N-2p and O-2p states.[12] Kitazawa[13] and Martínez-Ferrero[14] have studied N-doped mesoporous and mesostructured TiO_2 films after ammonia vapour treatment. For both, TiO_2 films treated in ammonia at 500 °C/2-4 h show enhanced photocatalytic activity, getting the optimum N substitution and maintaining the porous structure.

A large variety of methods have been developed to prepare TiO_2 films but sol-gel is the most widely used due to its facility to prepare films onto wide-area bodies at low temperature. The use of templates allows the self-assembly of organized micelles, and creates mesoporous films with high specific surface area. The textural and morphological properties greatly enhance the photocatalytic efficiency properties.[15,16] Different studies indicate that photocatalytic activity depends mainly on the total surface effectively irradiated with UV photons.[17]

The aim of this work was to prepare mesoporous nanocrystalline TiO_2-anatase films doped with Ca, W and N, using F127 and Brij58 as surfactants, to analyse the effect of dopants in the photocatalytic activity. Three dopants were selected: an anionic specie, N, that produces substitution of N at O sites, W as transition metal and Ca as alkaline-earth ions, both substituting Ti sites. The effect of dopants in the different parameters such as film thickness, total pore volume, specific surface area and total surface exposed to illumination was evaluated together with the photocatalytic activity through

the degradation of methyl orange. The analysis of textural properties permits to advance in the relationship between photocatalytic properties and film structure. The influence of dopants is important to explain the photocatalytic mechanisms inducing enhanced efficiency.

Experimental

Synthesis and characterisation of doped and un-doped TiO_2 sols

Doped TiO_2 sols were prepared using titanium isopropoxide (TISP, Aldrich, 284.22 g/mol, 97%) as precursor via acid catalysis. TISP was chemically modified by mixing with acetic acid (AcOH, Aldrich, 60.05 g/mol, 99.99%) or acetyl-acetone (AcAc, Merk, 100.12 g/mol, 99.5%), and absolute ethanol, in order to control the hydrolysis and condensation reactions. After 1 h of stirring, polyethylene glycol hexadecyl ether P5884 (Brij58, Aldrich, 1124 g/mol) was added to TISP/EtOH/AcOH solution, and Pluronic F-127 (F127, Aldrich, 12600 g/mol) to TISP/EtOH/AcAc one. Then, $Ca(NO_3)_2$ (Aldrich, 236.15 g/mol, 99%) was incorporated to TISP/EtOH/AcAc/F127 sol, while WCl_6 (Aldrich, 396.56 g/mol, 99.9%) was added to TISP/EtOH/AcOH/Brij58 sol with molar ratios $Ca(NO_3)_2$/TISP=0.03 and WCl_6/TISP=0.01. Finally, a mixture of ethanol and acidified water (0.1M HCl) was added drop by drop onto the solutions, up to reach a final oxide concentration of 30 g/L.

The final molar ratio was fixed to 1 TISP: 1 AcOH: 40 EtOH: 0.07 Brij58: 2 H_2O: (0.01-0.03) W/Ca, and 1 TISP: 1 AcAc: 40 EtOH: 5^*10^{-4} F127: 2 H_2O: (0.01-0.03) W/Ca. All the sols were aged for 2 days before coating deposition.

A reference TiO_2-AcOH-Brij58 and TiO_2-AcAc-F127 sols were prepared following the same process but without dopants addition.

The stability of the sols was studied through the evolution of viscosity with time, using an Ostwald viscometer (Pobel, 0c model, viscosity range 0.6-3 mPas).

Deposition of doped and un-doped TiO_2 films

Doped and un-doped TiO_2 thin films were deposited by dip-coating combined with Evaporation-Induced Self-Assembly (EISA) method onto glass-slides and silicon wafers. The films were obtained at 35 cm/min and 20% RH, and heat-treated in air at 450 °C for 1 h using a heating ramp of 10 °C/min. In the case of multilayer coatings, the same withdrawal rate was used along with an intermediate heat treatment of 350 °C/1 h between coatings followed by a final treatment of 450 °C for 1 h.

The glass-slides used to measure the photocatalytic activity were coated with one first layer of SiO_2, using a SiO_2 sol prepared in a two-step using TEOS (tetraethoxysilane).[18] SiO_2 coatings were sintered at 450 °C for 30 min, obtaining a thickness of ~210 nm, and a refractive index of ~1.44, corresponding to 98% of theoretical density of SiO_2. The quite dense SiO_2 coating avoids the diffusion of Na^+ cations from the glass substrate to the TiO_2 coating during firing and the possible inhibition of photocatalytic activity.[19,20]

Nitridation of TiO_2 films

Two layer TiO_2-AcOH-Brij58 films were nitrogen doped (N-doped) through nitridation treatments carried out in a tubular furnace using an anhydrous ammonia flow at 500 °C during 2 h. The treatment was performed increasing the temperature up to 500 °C in N_2 flow, then maintaining the sample in NH_3 flow for 2 h, and finally decreasing the temperature in N_2 atmosphere.

Characterisation of doped films

The coatings were characterised by optical microscopy (Zeiss, HP1, Germany) to detect the presence of precipitates, impurities, bubbles or cracks, and studied by transmission electronic microscopy (TEM) (Hitachi H-7100, Japan) to confirm the homogeneity and porous structure of the films. TEM samples were obtained by scratching the films and depositing the scaled fragments onto carbon-coated copper grids.

Ellipsometry and Environmental Ellipsometric Porosimetry (EEP) measurements were performed using a spectral Ellipsometer (M-2000UTM, J.A. Co., Woollam) modified with a system that allows controlling the relative humidity (RH) (Humidity Generator HG-1, Michel Instruments) to characterize films deposited onto glass-slides. The spectra were taken in the visible region, between 250 and 900 nm at a fixed incident angle of 70°. The data were fitted using the WVASE32 software with Cauchy model. From the fitting data, the refractive index (n) (taken at λ=700 nm) and the thickness (e) of the films were obtained as a function of relative humidity (from 0% to 100%). The total pore volume and the adsorption-desorption isotherms were further obtained by considering the Bruggeman Effective Medium Approximation model (BEMA). The pore size distributions were calculated utilizing a modified Kelvin equation taking into account ellipsoidal pore geometry.[21] Finally, an estimation of the specific surface area and the exposed surface area per cm^2 of sample were calculated.

Coatings deposited onto silicon wafers were analyzed by Fourier transform infrared spectroscopy (FTIR) to follow the elimination of surfactants and the crystallization of anatase. FTIR spectra were recorded in transmission mode in the frequency range 4000-400 cm^{-1} with a resolution of 2 cm^{-1} using a Perkin Elmer FTIR Spectrum 100 equipment.

The hydrophobic/hydrophilic character of coatings was evaluated through the contact angle using an Easy Drop equipment ("Drop Shape Analysis System" Kruss DSA 100).

Grazing incidence X-ray diffraction (GXRD) studies were performed on films deposited onto silicon wafers using Cu$K\alpha$ radiation in a Panalytical diffractometer (X'Pert PRO theta/theta) for analysing the crystallisation of TiO_2-anatase. The diffractrograms were recorded in the range of 2Θ=20-70°, using a fixed counting time of 20 s/step and an increment of 0.05°.

Finally, the photocatalytic activity was evaluated by the degradation of methyl orange (MO) in aqueous solution using the films deposited onto glass-slides on top of a first layer of SiO_2. The light sources system consists of three UV-lamps of

6W with a maximum emission at 365 nm wavelength (Philips F/TL/6W/08, Holland).

The measurements were performed using 50 mL of an aqueous solution of methyl orange (MO) with a concentration c=3 mg/L. The pH of the solution was adjusted to 2 using HCl[22] and the total surface tested was equal to 50 cm^2. The reactor vessel containing the solution was covered with window-glass to prevent solution evaporation. First, photolysis and dark tests (adsorption) were performed to confirm that the degradation of MO is associated to the TiO_2 film and not to light irradiation and/or adsorption.

Photocatalytic measurements were performed introducing TiO_2 samples in the MO solution and maintained under continuous stirring and irradiation. Aliquots of 1mL were collected every 10 min and analysed by spectrophotometry UV/vis (UV-vis, Perkin Elmer, Lambda 950), evaluating the degradation of MO through the diminution of the absorption band at 508 nm.

Results and discussion

Doped TiO_2 sols and films characterisation

Homogeneous and transparent doped and un-doped sols were obtained for both compositions TiO_2-AcAc-F127 and TiO_2-AcOH-Brij58. The sols prepared with AcAc are yellow, the rest being colourless.

The stability of doped and un-doped TiO_2 sols was evaluated through viscosity measurements at 25 °C as a function of aging time. In all the cases, a Newtonian behaviour was observed with initial viscosities between 1.5 and 2 mPa.s, not changing with the aging time for at least 1 month, thus revealing an excellent stability. The doping does not affect the stability of TiO_2 sols.

TiO_2 films were deposited onto glass-slides and Si-wafers from doped and un-doped TiO_2-AcAc-F127 and TiO_2-AcOH-Brij58 sols. After the heat-treatment good optical quality, transparency without precipitates and excellent adherence and mechanical stability were observed for all the coatings.

The crystallisation of the inorganic network as TiO_2 anatase was confirmed by GXRD. Figure 1 shows the GXRD patterns of TiO_2-AcAc-F127, TiO_2-AcOH-Brij58 and the same compositions doped with Ca.

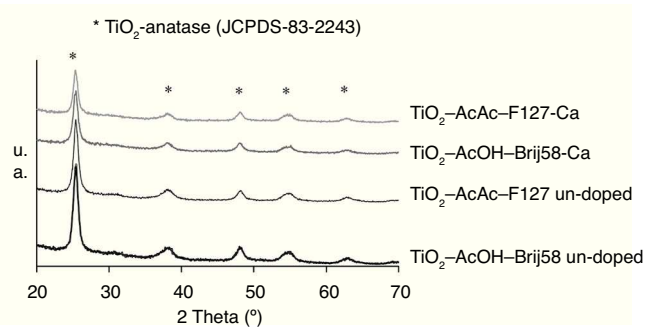

Figura 1 – XRD spectra of Ca-doped and un-doped mesoporous TiO_2 films.

For all the coatings, tetragonal TiO_2-anatase phase (JCPDS-00-083-2243) was identified as only phase, rutile or brookite phases not appearing. For Ca-TiO_2-coatings, no calcium oxide impurity phases were detected likely due to the small concentration of Ca^{2+} incorporated. For the films doped with W and N the same effect was observed (not shown). However, the doping of TiO_2 affects the crystallinity, decreasing the intensity peaks. Using the Scherrer´s equation the particle size (D) of TiO_2 coatings were calculated obtaining values between 9.6 and 10 nm. These results indicate that the dopant does not affect the crystal size but the crystal fraction tends to decrease.

The crystal parameters have been calculated considering a tetrahedral crystal structure (Table 1). The doping of TiO_2 produced some distortion in the lattice of TiO_2. For Ca and W doped TiO_2 the lattice parameter "a" decreases, increasing the "c" parameter. Depending on the ionic radius of the dopant, it can be introduced substitutionally or interstitially in the matrix. In all the cases, a deformation of the tetrahedron is observed. R. Rodriguez-Talavera et al.[23] report that if the size of the dopant is larger than titanium but smaller than oxygen, such as Ca^{2+} (0.99 Å), the dopant is introduced substitutionally in the matrix, producing an oxygen deficiency in the crystal and stabilizing the anatase phase. Thus, the elongation of the tetrahedron obtained in our case could be explained considering the introduction of Ca^{2+} in substitution Ti^{4+} sites in the TiO_2 lattice. For W^{6+}, the ionic radius (0.64 Å) is very similar to Ti^{4+} (0.68 Å) whereas the charge of the ion dopant is higher. In this case, the excess of charge produces a similar effect that the ion size. The W^{6+} is introduced substitutionally in the TiO_2 matrix, deforming the structure due to the electric field created between the dopant and the surrounding ions.[23]

The FTIR spectra (not shown), revealed that C-H and C-O vibrations of Brij58 and F-127 did not appear, confirming that templates have been totally removed and TiO_2 matrix is fully crystallized in anatase form after the heat treatment.

Nitrided TiO_2-AcOH-Brij58 films were homogeneous, transparent, crack free and slightly yellowish. The crystallisation of TiO_2 in anatase phase was confirmed by XRD and crystal sizes around 10 nm were determined, indicating that nitridation treatment does not affect the crystal size compared with un-doped films. The lattice parameter "a" does not change with the nitridation however the "c" axis increases (Table 1). The defect of charge of N^{3-} respecting to the substituted O^{2-} in the anatase network likely explained the deformation of the structure.

Textural characterisation of TiO_2 films

Spectral Ellipsometry and Environmental Ellipsometric Porosimetry (EEP) measurements were used to determine the thickness, refractive index and porosity properties of the films.

Table 2 summarizes the thickness (e) and refractive index (n) of the coatings. Doped TiO_2 films show lower thickness and similar refractive index than those of un-doped films, except to N-doped film in which the nitridation treatment

Table 1 – Crystal parameters and kinetics constants of un-doped and doped photocatalysts

Composition	Lattice parameters (Å)		k (k/min)	K`(k/S_{exp})
	a(+/–0.0025)	c (+/–0.0025)		
TiO_2-A-AcOH-Brij58	3.787	9.437	0.0052	0.000086
TiO_2-A-AcOH-Brij58-Ca	3.768	9.472	0.0091	0.00015
TiO_2-A-AcOH-Brij58-W	3.777	9.473	0.0185/0.0031	0.00033/0.000056
TiO_2-A-AcOH-Brij58-N	3.785	9.472	0.005	0.00018
TiO_2-A-AcAc-F127	3.783	9.431	0.0048	0.000084
TiO_2-A-AcAc-F127-Ca	3.786	9.460	0.0114	0.000178
TiO_2-A-AcAc-F127-W	3.777	9.472	0.007/0.0013	0.00012/ 0.000022

Table 2 – EEP characterisation for doped and un-doped TiO_2 films

	Composition	e(nm) ±2	n ±0,05	V_{pore}(%) ±5%	ϕ(nm) ±10%	S_s(m^2/cm^3) ±10%	S_{exp}(cm^2) ±10%	θ (º)
TiO_2-AcOH-Brij58	Un-doped	340	1.77	32	3	194	57	27
	Ca	310	1.74	34	7.8	124	58	9.5
	W	290	1.75	33	2-12 *	161**	55	18
	N-doped	260	1.79	26	13	69	26	22
TiO_2-AcAc-F127	Un-doped	303	1.73	20	6-11	175	57	28
	Ca	263	1.79	17	6-12*	170*	64	7.6
	W	273	1.76	16	2-11*	160**	58	9.1

* Bimodal distribution
** S_s medium

slightly increases the refractive index and decreases the thickness because of an extra thermal treatment. Figure 2a and 2b shows the thickness and the refractive index of a TiO_2-AcAc-F127-Ca film at λ=700 nm, as a function of RH during adsorption and desorption measurements.

At low RH, low values of refractive index (n=1.73) were obtained, which is characteristic of the presence of high porosity. When RH increases, the thickness and the refractive index remain near constant up to 50%. At this humidity, a sharp increase of refractive index and a simultaneous

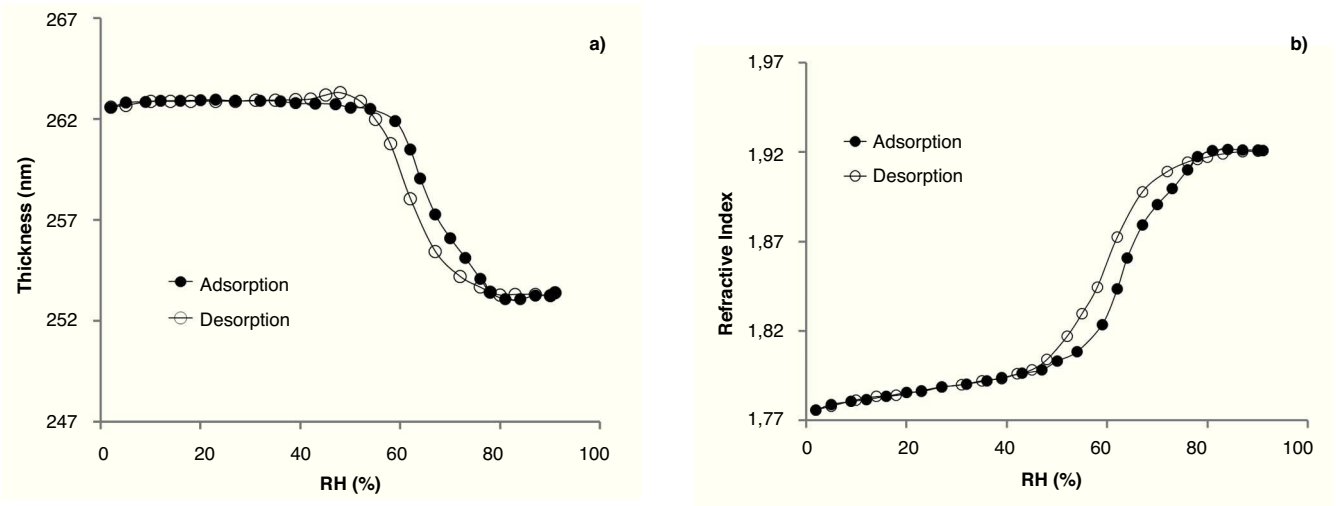

Figura 2 – Variation of thickness (a) and refractive index (b) of TiO_2 -AcAc -F127-Ca film as a function of RH.

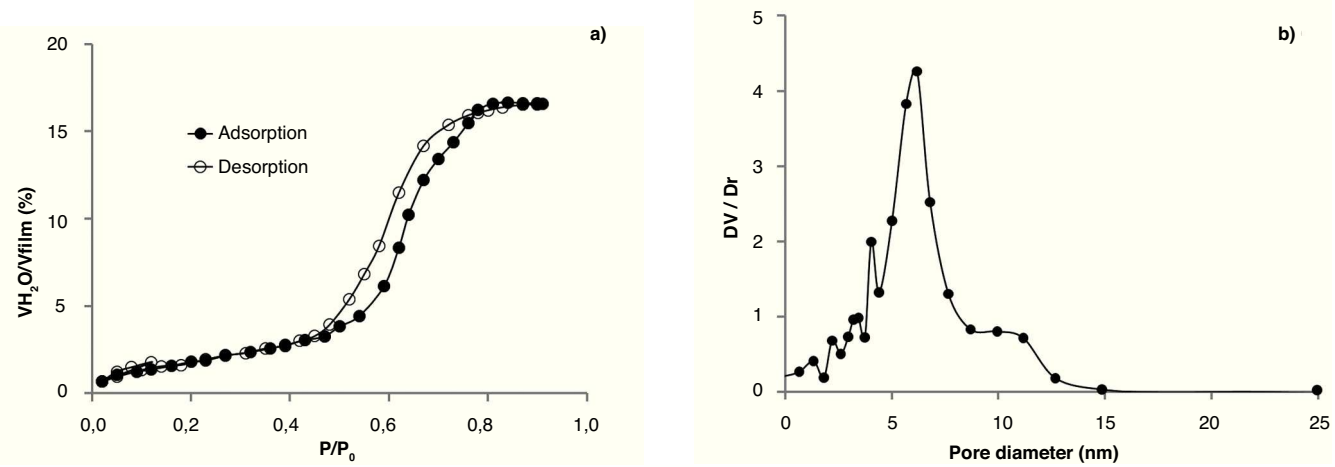

Figura 3 – Adsorption/desorption isotherm (a) and pore size distribution (b) for TiO_2 -AcAc -F127-Ca film.

decrease in thickness is observed, indicating the capillary water condensation into the pores and the corresponding filling of them.[21] After the first adsorption/desorption cycle, the refractive index and the thickness reached the original values indicating that the film is stable during all the adsorption and desorption process.

The total pore volume in dry air and the full isotherms were calculated by using BEMA model and the pore size distribution using the Kelvin's equation modified. Figure 3a and 3b shows the water adsorption/desorption isotherms and the pore size distribution for a TiO_2-AcAc-F127-Ca film. A reversible type IV-adsorption/desorption isotherm with hysteresis loop is observed (Fig. 3a), indicating the presence of pores in the mesoporous range (2-50 nm). TiO_2-AcAc-F127-Ca films present a total pore volume of 17% (Fig. 3a) and a bimodal pore size distribution between 6.2 and 10 nm (Fig. 3b).

The rest of samples exhibit isotherms with similar shapes. All the films presented total pore volume (V_{pore}) between 33 and 16%, and pore size between 3 y 13 nm (Table 2). TiO_2-A-AcOH-Brij58-W, TiO_2-A-AcAc-F127 and TiO_2-A-AcAc-F127-Ca films present bimodal pore size distributions with values around 2 and 12 nm.

The specific surface area (S_s) together with the exposed area (S_{exp}) was calculated,[17,21,24] (Table 2). This last parameter represents the total area exposed to irradiation, thus being relevant for photocatalytic behaviour.

All the doped TiO_2 films present lower values of contact angle (Θ) than un-doped coating, showing that dopants increase the hydrophilicity of the films; this behaviour agrees with the results reported by Yuan et al.[25]

The textural properties are summarised for doped and un-doped TiO_2 films in Table 2 together with the contact angle.

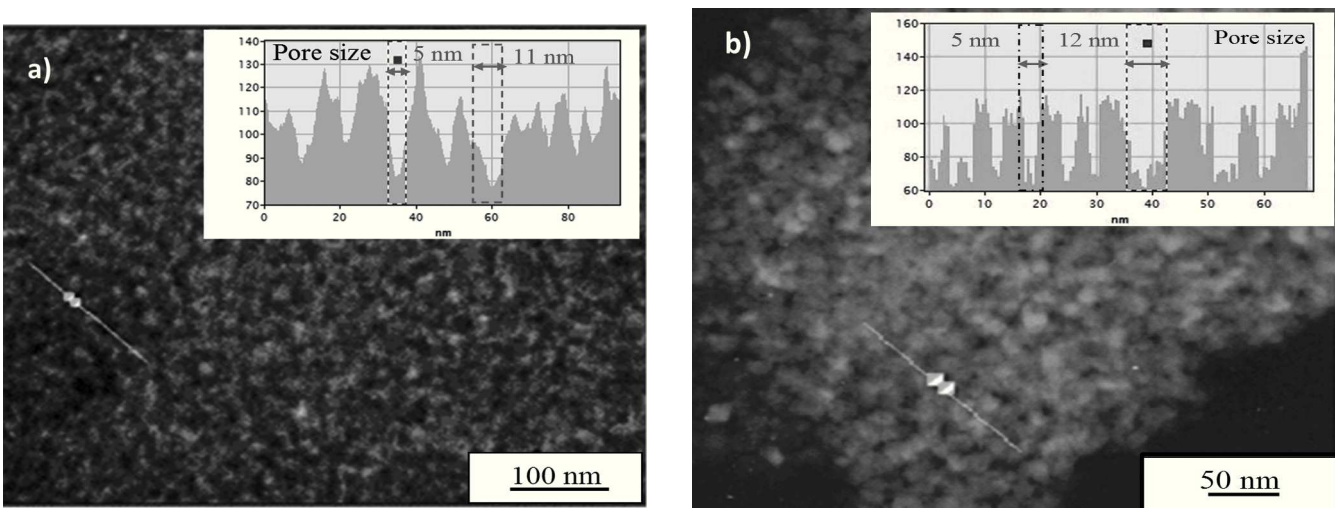

Figura 4 – TEM micrographs of films TiO_2 -AcAc -F127 (a) and TiO_2 -AcAc-F127 Ca-doped (b).

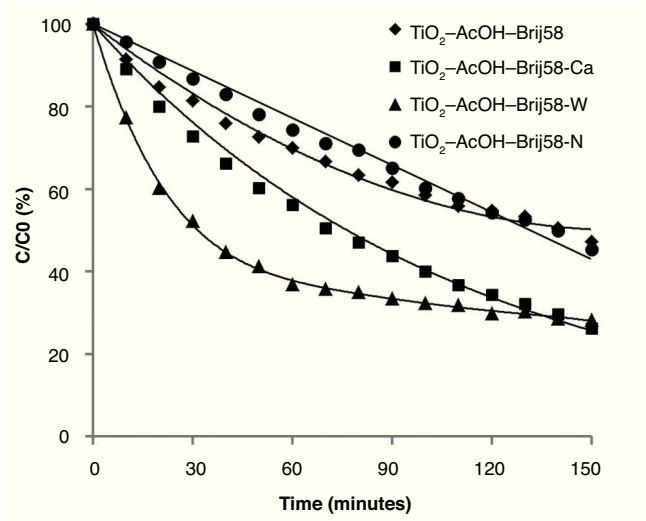

Figura 5 – Photocatalytic degradation of methyl orange (c=3 mg/L) for doped and un-doped TiO_2 -AcOH-Brij58 films.

Transmission electronic microscopy (TEM) was used to confirm the porous structure of the coatings. Figure 4 shows the micrographs of TiO_2-AcAc-F127 un-doped and TiO_2-AcAc-F127-Ca films. TiO_2-AcAc-F127 un-doped film shows a high porosity with bimodal pore size distribution around 5 and 11 nm, but without any order. On the other hand, TiO_2-AcAc-F127-Ca film presents a similar structure, with slightly higher bimodal pore size around 5 and 12 nm. These results confirm the porosity characterisation obtained by EEP.

UV-visible spectra were used to determine the band-gap of TiO_2 films. The $E_{band\text{-}gap}$ can be calculated through equation 1 by fitting the linear relation of $(\alpha E)^{1/m}$ versus E plot.

$$(\alpha E)^{1/m}=A(E_{ban\text{-}gap}-E_g) \quad (1)$$

α is the absorption coefficient, E_g is the energy of a photon, A is a constant, and m is the parameter that depends on the electronic transition of the semiconductor; for indirect transition semiconductor such as TiO_2-anatase phase m=2.[26] The calculated band gap of undoped-TiO_2 film is 3.5 eV shifting to 3.4 or 3.3 eV for doped TiO_2 films.

The incorporation of Ca or W dopants produces a slight displacement of the band gap likely to due intermedium states created within the band gap according to data observed by R. Long and N. J. English.[27]

Photocatalytic activity of TiO_2 films

The photocatalytic activity of doped and un-doped TiO_2 films was evaluated by studying the degradation of methyl orange (MO).[22] The preliminary tests show that neither photolysis nor adsorption process occur.

The photocatalytic behaviour of TiO_2-AcOH-Brij58 films with and without dopant was first analysed (Fig. 5).

The study revealed that the photocatalytic activity of TiO_2 films was greatly enhanced by Ca^{2+} and W^{6+} doping. TiO_2-AcOH-Brij58-Ca and TiO_2-AcOH-Brij58-W films show a decomposing of 72% of MO after 2.5 h under UV irradiation. Even though the final degradation is similar for both dopants, the kinetic behaviour is different. W-doped-TiO_2 degrades up to 60% of MO after 50 min of irradiation whereas TiO_2-AcOH-Brij58-Ca reaches only 40%. This indicates that the TiO_2-AcOH-Brij58-W film is initially more active but the active sites could be further blocked by dye ions, thus decreasing the degradation rate. In this case, the kinetic process can be divided in two steps. For obtaining the kinetic parameters, the photocatalytic decomposition of MO was described by a first order kinetic model.[28] $\ln (C_0/C)=kt$, where C_0 and C is the concentration at t=0 and at time t. The plots of $\ln (C_0/C)$ *vs* t show a straight line the slope k (Fig. 6). Table 2 shows the first order rate constants, k, together with the normalized rate constants, K' defined as $K'=k/(S_{exp})$ for the different TiO_2 films used in this study.

On the other side, k value parameter of TiO_2-AcOH-Brij58-Ca film was the maximum even after it was normalized per surface area. Un-doped and TiO_2-AcOH-Brij58-W films show similar degradation rate, 0.005 k/min, but TiO_2-AcOH-Brij58-W film shows two different behaviours. For degradation times lower than 50 min, a high kinetic rate (0.0185 k/min) is obtained, even higher than that of TiO_2-AcOH-Brij58-Ca film. However, the photocatalytic process drops sharply from this time and the reaction rate decreases up to 0.0031 k/min, which is associated with the blocking or saturation of the active sites.

In order to explain the photocatalytic behaviour, two aspects should be considered, one associated with the nature of the dopant and other with the textural and porous structure of the coatings. In the case of Ca^{2+} ion, the dopant enters in the lattice substituting Ti^{4+} and induces oxygen vacancies, increasing the active sites. Furthermore, W^{6+} ions could easily replace Ti^{4+} (similar ionic radii) but causing an excess of

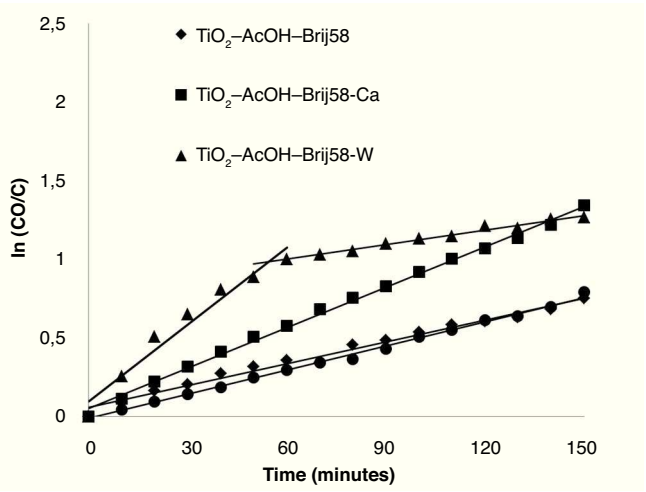

Figura 6 – First-order kinetics for methyl orange degradation for doped and un-doped TiO_2 -AcOH-Brij58 films.

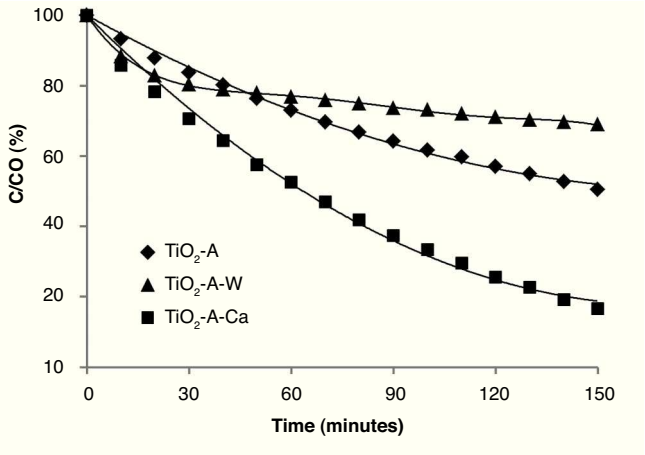

Figura 7 – Photocatalytic degradation of methyl orange (c=3 mg/L) for doped and un-doped TiO_2 -AcAc-F127 films.

positive charge on the network. Both effects can reduce the recombination e^-/h^+ pairs, acting as bridge for electron transition and increasing the photocatalytic activity.[29,30]

The other aspect affecting the photocatalytic activity is associated with the porosity (Table 2) of Ca and W doped films. TiO_2-AcOH-Brij58-Ca films present a small pore size associated with high specific surface area (S_s). Chen and Dionysiou[31] demonstrated that photocatalysts with pore size around 5 nm show higher photocatalytic degradation rates. On the other hand, TiO_2–AcOH-Brij58-W coatings show a bimodal pore size distribution. The smaller pores are initially more active, but will rapidly saturate by adsorption of MO molecules thus causing the decrease in photocatalytic activity.

Considering the first aspect (nature of dopant), TiO_2-AcOH-Brij58-W film should have high photocatalytic activity, but the textural properties reduce this activity. However, for Ca-doped TiO_2 films both factors affect positively promoting enhanced photocatalytic performance.

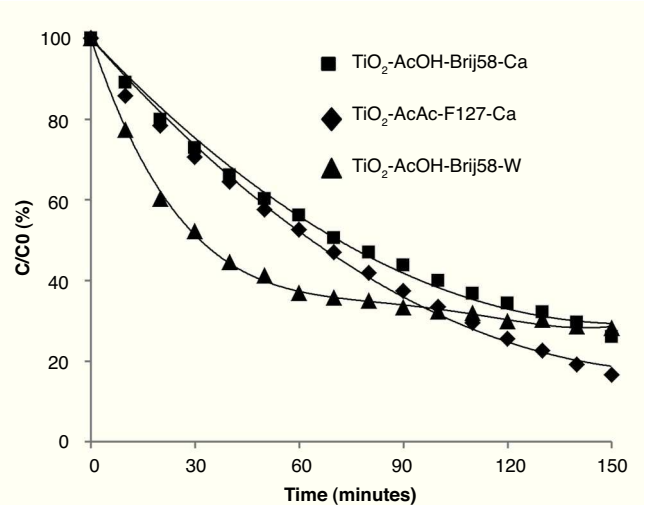

Figura 8 – Best photocatalytic results for doped TiO_2 films studied by methyl orange degradation.

Finally, TiO_2-AcOH-Brij58-N films show similar photocatalytic efficiency that un-doped TiO_2-AcOH-Brij58 film because the nitridation treatment provokes the partial collapse of the porosity structure of the coatings, S_s of 69 m^2/cm^2 versus 194 m^2/cm^2, this reducing drastically the efficiency. Thus the effect of N as dopant is counteracted by the reduction of porosity and S_s.

TiO_2-AcAc-F127 films were also evaluated (Fig. 7). In this case, Ca-doped TiO_2-AcAc-F127 film shows the highest photocatalytic efficiency, decomposing 83% of MO after 2.5 h of UV irradiation, followed by un-doped film. The photocatalytic behaviour of Ca as dopant is similar to that of TiO_2-AcOH-Brij58-Ca film with the highest k constant rate, 0.0114 k/min. As in the previous case, W-doped presents two different steps during the irradiation time. The results reveal a rapid degradation of MO at initial radiation time, with a k value of 0.007 k/min, followed by a sharp decrease of the degradation rate down to 0.0013 k/min. Analogous arguments can explain the best photocatalytic activity of the catalyst. Ca-doped films present a pore size around 6 nm and high S_s (m^2/cm^3) that, together with the introduction of the Ca^{2+} ions in the TiO_2 matrix, contributes to obtain the best photocatalytic behaviour, avoiding the recombination of e^-/h^+ pairs.

Figure 8 compares the best photocatalytic results obtained for TiO_2 films. The highest photocatalytic efficiencies were obtained for films doped with Ca and W associated with their textural properties: small pore size (6 nm) and high specific surface area, together with the effect of the incorporation of the dopant into the TiO_2 matrix substituting Ti^{4+} ions in the anatase network.

The textural properties, particle size and specific surface area of the TiO_2 films, as well as the chemical nature, size and charge of the dopants, are all key factors affecting the photocatalytic properties and determining the efficiency of the catalysts.

The much enhanced efficiency of Ca^{2+} and W^{6+} doped mesoporous titania films convert these materials in appropriated candidates for in-door and out-door applications.

Conclusions

TiO_2 mesoporous films with much enhanced photocatalytic activity were prepared by doping with Ca and W ions. Anatase was the only identified phase in all the photocatalysts, whether doped or un-doped.

The doping of TiO_2 affects the crystallinity provoking the decrease of the peak intensity. The calculated crystal size of TiO_2-anatase is around 10 nm in all the coatings, indicating that the dopant does not affect the crystal size but the crystal fraction tends to decrease.

The introduction of Ca^{2+} or W^{6+} ions produces some distortion in the unit cell dimension of TiO_2. The lattice parameter "a" decreases, and the "c" parameter increases for doped TiO_2 films.

The pore volume and pore size values vary between 33 and 16% and 3 y 13 nm, respectively. Moreover, TiO_2-AcAc-F127 films with and without dopants present bimodal porosity greatly affects the photocatalytic performance.

TiO_2-AcOH-Brij58-W films show higher photocatalytic activity at initial UV radiation time; however, the saturation of the smaller porosity reduces the activity. For Ca-doped films, the adequate textural properties (pore size and high S_s) and the introduction of Ca^{2+} ions in substitutional positions of Ti^{4+} in the TiO_2 matrix contributes positively to obtain a much enhanced photocatalytic activity.

Ca^{2+} ions enter in the lattice substituting Ti^{4+} and inducing oxygen vacancies that increase the active sites. Furthermore, W^{6+} ions could easily replace Ti^{4+} (similar ionic radii) but causing an excess of positive charge on the network. Both effects can reduce the recombination e^-/h^+ pairs, acting as bridge for electron transition and increasing the photocatalytic activity.

On the other hand, the nitridation process produces the partial collapse of the TiO_2 matrix being detrimental for the photocatalytic activity.

Textural properties, particle size and specific surface area, as well as chemical nature, size and charge of the dopants are key factors affecting the photocatalytic properties.

The much enhanced efficiency of Ca^{2+} and W^{6+} doped mesoporous titania films convert these materials in appropriated candidates for in-door and out-door applications.

Acknowledgements

The work was supported by PIE-CSIC-2004-60E637. The authors also acknowledge Laura Peláez and Aritz Iglesias for the experimental work.

REFERENCES

1. Legrini, O.; Oliveros, E.; Braun, A.M., (1993): Photochemical processes for water treatment, *Chem. Rev.,* 93(2): 671-698. http://dx.doi.org/10.1021/cr00018a003.
2. Dvoranová, D.; Brezová, V.; Mazúr, M.; Malati, M. A., (2002): Investigations of metal-doped titanium dioxide photocatalysts, *Appl. Catal. B Environ.,* 37:91-105. http://dx.doi.org/10.1016/S0926-3373(01)00335-6.
3. Yang, Y.; Li, X.-J.; Chen, J.- T.; Wang, L.-Y.; (2004): Effect of doping mode on the photocatalytic activities of Mo/TiO_2, *J. Photoch. Photobio. A,* 163:517-522. http://dx.doi.org/10.1016/j.jphotochem.2004.02.008.
4. Xu, J.; Ao, Y.; Chen, M.; Fu, D.; Yuan, C., (2010): Photocatalytic activity of vanadium-doped titania–activated carbon composite film under visible light, *Thin Solid Films,* 518:4170-7174. http://dx.doi.org/10.1016/j.tsf.2009.12.005.
5. Choi, W.; Termin, A.; Hoffmann, M.R., (2006): The Role of Metal Ion Dopants in Quantum-Sized TiO_2: Correlation between Photoreactivity and Charge Carrier Recombination Dynamics, *J. Phys. Chem.,* 98(51):13669-13679. http://dx.doi.org/10.1021/j100102a038.
6. Zhu, J.; Deng, Z.; Chen, F., (2006): Hydrothermal doping method for preparation of Cr^{3+}-TiO_2 photocatalysts with concentration gradient distribution of Cr^{3+}, *Appl. Catal. B: Environ.,* 62(3-4):329-335. http://dx.doi.org/10.1016/j.apcatb.2005.08.013.
7. Žabova, H.; Sobek, J.; Církva, V.; Šolcova, O.; Kment, #S.; Hájek, M., (2009): Efficient preparation of nanocrystalline anatase TiO_2 and V/TiO_2 thin layers using microwave drying and/or microwave calcination technique, *J. Solid State Chem.,* 182(12):3387-3392. http://dx.doi.org/10.1016/j.jssc.2009.09.033.
8. Yang, Y.; Wang, H.; Li, X.; Wang, C., (2009): Electrospun mesoporous W^{6+}-doped TiO_2 thin films for efficient visible-light photocatalysis, *Mater. Lett.,* 63:331-333. http://dx.doi.org/10.1016/j.matlet.2008.10.037.
9. Rampual, A.; Parkin, I.P. ; O´Neill, S.A.; Desouza, J.; Mills, A.; Elliott, N., (2003): Titania and tungsten doped titania thin films on glass; active photocatalysts, *Polyhedron,* 22:35-44. http://dx.doi.org/10.1016/S0277-5387(02)01333-5.
10. Al-Salim, N.I.; Bagshaw, S.A.; Bittar, A.; Kemmitt, T.; Macquillan, A.J.; Millsa, A.M.; Ryana, M J., (2000): Characterisation and activity of sol–gel-prepared TiO_2 photocatalysts modified with Ca, Sr or Ba ion additives, *J. Mater. Chem.,* 10(10):2358-2363. http://dx.doi.org/10.1039/b004384m.
11. Asahi, R.; Morikawa, T.; Ohwaki, T.; Aoki, K.; Taga, Y., (2001): Visible-Light Photocatalysis in Nitrogen-Doped Titanium Oxides, *Science,* 293:269-271. http://dx.doi.org/10.1126/science.1061051.
12. Chekini, M.; Mohammadizadeh, M.R.; Vaez Allaei, S.M., (2011): Structural and electrical properties of evaporated Fe thin films, *Appl. Surf. Sci.,* 257: 7179-7183. http://dx.doi.org/10.1016/j.apsusc.2011.03.084.
13. Kitazawa, N.; Sato, H.; Watanabe, Y., (2007): Effects of post-deposition chemical treatment on the formation of mesoporous titania films, *J. Mater. Sci.*, 42:5074-5085. http://dx.doi.org/10.1007/s10853-006-0479-8.
14. Martínez- Ferrero, E.; Sakatani, Y.; Boissiere, C.; Grosso, D.; Fuertes, A.; Fraxedas, J.; Sánchez, C., (2007): Nanostructured Titanium Oxynitride Porous Thin Films as Efficient Visible-Active Photocatalysts, *Adv. Funct. Mater.,* 17:3348-3354. http://dx.doi.org/10.1002/adfm.200700396.
15. Sakatani, Y.; Grosso, D.; Nicole, L.; Boissière, C.; Soler-Illia Galo, J. de A.A.; Sanchez, C.; (2006): Optimised photocatalytic activity of grid-like mesoporous TiO_2 films: effect of crystallinity, pore size distribution, and pore accessibility, *J. Mater. Chem.,* 16:77-82. http://dx.doi.org/10.1039/b512824m.
16. Arconada, N.; Castro, Y.; Durán, A. ; Héquet, V., (2011): Photocatalytic oxidation of methyl ethyl ketones over sol–gel mesoporous and meso-structured TiO_2 films obtained by EISA method, *Appl. Catal. B: Environ.*, 107(1-2):52-58. http://dx.doi.org/10.1016/j.apcatb.2011.06.036.
17. Arconada, N.; Castro, Y.; Durán, A., (2010): Photocatalytic properties in aqueous solution of porous TiO_2-anatase films prepared by sol-gel process, *Appl. Catal. A: General,* 385 (1-2):101-107. http://dx.doi.org/10.1016/j.apcata.2010.06.051.
18. Guglielmi, M.; Brusatin, G.; Tombolan. N., (1993): Ion migration in thin sol-gel glass coatings, *Riv. Staz. Sper. Vetro Sup.*, 23:495-498.
19. Nam, H.-J.; Amemiya, T.; Murabayashi, M.; Itoh, K., (2004): Photocatalytic Activity of Sol-Gel TiO_2 Thin Films on Various Kinds of Glass Substrates: The Effects of Na^+ and Primary Particle Size, *J. Phys. Chem. B,* 108:8254-8259. http://dx.doi.org/10.1021/jp037170t.
20. Oh, S. H. ; Kim, J. S.; Chung, J. S.; Kim, E. J.; Hahn, S. H., (2005): Crystallization and Photoactivity of TiO_2 Films Formed on Soda Lime Glass by a Sol-Gel Dip-Coating Process, *Chem. Eng. Commun.,* 192(3):327-335. http://dx.doi.org/10.1080/00986440590473524.
21. Boissiere, C.; Grosso, D.; Lepotre, S.; Nicole, L.; Brunet, A.B.; Sánchez, C., (2005): Porosity and Mechanical Properties of Mesoporous Thin Films Assessed by Environmental Ellipsometric Porosimetry, *Langmuir*, 21:12362-12371. http://dx.doi.org/10.1021/la050981z.

22. Wang, W.; Tao, J.; Wang, T.; Wang, L., (2007): Photocatalytic activity of porous TiO_2 films prepared by anodic oxidation, *Rare Metals*, 26(2):136-141. http://dx.doi.org/10.1016/S1001-0521(07)60173-9.
23. Rodríguez-Talavera, R.; Vargas, S.; Arroyo-Murillo, R.; Montiel-Campos, R.; Haro-Poniatowski, E., (1997): Modification of the phase transition temperatures in titania doped with various cations, *J. Mater. Res.,* 12:439-443. http://dx.doi.org/10.1557/JMR.1997.0065.
24. Arconada, N.; Castro, Y.; Duran, A.; Héquet, V., (2011): Photocatalytic oxidation of methyl ethyl ketones over sol–gel mesoporous and meso-structured TiO_2 films obtained by EISA method, *Appl. Catal. B: Environ.,* 107:52-58. http://dx.doi.org/10.1016/j.apcatb.2011.06.036.
25. Yuan, Z.; Zahng, J.; Li, B.; Li, J., (2007): Effect of metal ion dopants on photochemical properties of anatase TiO_2 films synthesized by a modified sol-gel method, *Thin Solid Films,* 515:7091-7095. http://dx.doi.org/10.1016/j.tsf.2007.02.101.
26. Martínez, S.; Serrano, T.; Gómez, I.; Hernández, A., (2007): Síntesis y caracterización de nanoparticulas de CdS obtenidas por microondas, Bol. Soc. Esp. Ceram. Vidr. 46(2):97-101. http://dx.doi.org/10.3989/cyv.2007.v46.i2.256.
27. Long, R.; English, N. J., (2011): Giant mesoscopic photoconductance fluctuations in Ge/Si quantum dot system, *Appl. Phys. Letters*, 98:142101-142103. http://dx.doi.org/10.1063/1.3574022.
28. Rashed, M. N.; El-Amin, A. A., (2007): Photocatalytic degradation of methyl orange in aqueous TiO_2 under different solar irradiation sources, *Int. J Phys. Sci.,* 2(3):73-81.
29. Li, X.Z.; Li, F.B.; Yang, C.L.; Ge, W.K., (2001): Bond cleavage in the excited state of acyl phosphene oxides: Insight on the role of conformation by model calculations: a concept, *J. Photochem. Photobiol. A-Chem.*, 141(2-3):209-217. http://dx.doi.org/10.1016/S1010-6030(01)00446-4.
30. Bosc, F.; Edward, D.; Keller, N.; Keller, V.; Ayral, A., (2006): Mesoporous TiO_2-based photocatalysts for UV and visible light gas-phase toluene degradation, *Thin Solid Films,* 495 (2006) 272-279. http://dx.doi.org/10.1016/j.tsf.2005.08.361.
31. Chen, Y.; Dionysiou, D.D., (2006): Correlation of structural properties and film thickness to photocatalytic activity of thick TiO_2 films coated on stainless steel, *Appl. Catal. B: Environ.,* 69:24-33. http://dx.doi.org/10.1016/j.apcatb.2006.05.002.